Optica Applicata, Vol. XXIV, No. 3, 1994

Two-wavelength spatial filtering based system for prescreening of cervical smears

D. LITWIN

Institute of Applied Optics, ul. Kamionkowska 18, 03–805 Warszawa, Poland.

An experimental system for identification of early cervical pathology in mass examination of women is presented. It uses band-pass spatial frequency filtering technique for the fast localization of atypical cells by transforming their dark stained nuclei into bright spots whose intensities depend on the nuclei diameter. The nuclei of enlarged size, which are the symptom of the disease, are detected by measuring the intensity level of the spots. This paper is focused on the problem of artifacts rejection by dual wavelength illumination and coherent noise suppression.

1. Introduction

Cancer of the uterine cervix often develops into invasive carcinoma without giving any symptoms and cannot be diagnosed by gross examination. When it is possible to observe the symptoms, it may be too late for a successful treatment. The disease it a major source of premature female mortality. For example, in the United Kingdom the number of deaths exceeded two thousand in 1987 [1]. Cervical cancer in its noninvasive stage can be detected by inspecting a sample of cells taken from the cervix under a microscope. Studies all over the world show that for women who have been tested regularly, the death rate is significantly reduced [2]–[6]. The incidence of cervical carcinoma decreased 3 times in Sweden when women were screened only once during ten years [7]. These reports indicate that to reduce the number of death cases every woman should be examined every second or third year. Searching for abnormal cells requires experience and close acquaintance with cytological details. Because of lack of highly trained cytotechnicians the introduction of the mass screening program has small chance of success. Over the last three decades many fully or partially automated prescreening systems have been designed to overcome this restriction [1]. Both digital [8]–[12] and hybrid optodigital [13], [14] techniques of image processing have been used or proposed including flow systems [15]–[17].

An advanced digital analysis of cell features, because of large variability of cell types, must be performed on a high resolution (HR) image – typically pixel

---

* This paper is a revised and extended version of a paper presented at the *SPIE International Conference on Holography, Interferometry and Optical Pattern Recognition in Biomedicine III, Biomedical Optics'93*, January 1993, Los Angeles. The conference version of this paper appeared in SPIE Proceedings 1889 (1993), 70.

size is equal to 0.25 μm. From the economical point of view, processing of entire sample in HR mode is not efficient because in mass examination a majority of cells are normal. A large number of objects and a limited processing area would make such a procedure time consuming [18]. Instead, searching for cells is divided into low (LR) and high resolution (HR) steps. HR analysis is restricted only to suspect objects detected in LR stage (pixel size is equal to 2–4 μm). This strategy is similar to that used by cytologists and has been used in previously developed automated systems [11].

The LR step may be implemented either digitally or optically. This paper concerns optical band-pass filtering for performing this task.

2. Spatial filtering technique

Three successive operations create the spatial filtering technique: Fourier transformation of the image (FT), its spectrum modification by the spatial filter, inverse Fourier transformation (FT^{-1}).

Cancerous cells are described by a set of features. The nucleus of an enlarged diameter is one of them. Applying a suitable band-pass filter dark nuclei are con-

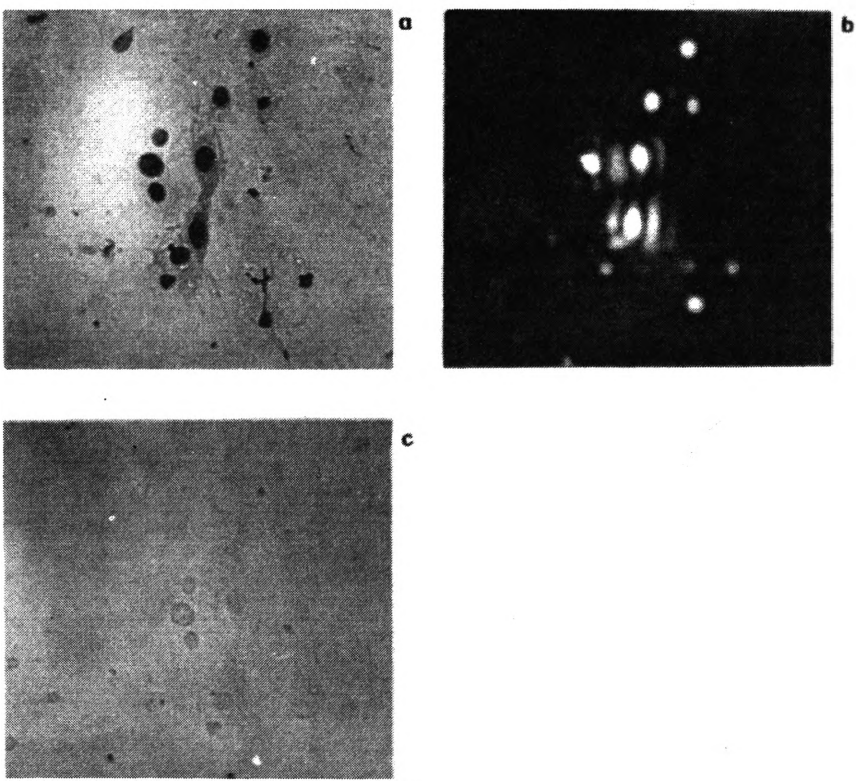

Fig. 1. Images of a pathological cervical smear (photographs taken from the computer monitor). a – direct image (600 nm), b – filtered image (633 nm), c – direct image (890 nm)

verted into bright spots located on a dark background (Fig. 1 **a, b**). The intensities of the spots depend on the nuclei diameters and can easily be measured. If transfer characteristic of the filter is adjusted so that it reaches its maximum for these enlarged nuclei, they can be easily selected without classical segmentation. The optical filtering technique has the following advantages:

– optical Fourier transformation does not depend on pixel size and the number of pixels taken for calculation, therefore the larger area may be processed without loss of accuracy which consequently speeds up the analysis;

– it is faster than digital transformation;

– analysis of filtered images needs less precise focusing because only intensities of spots are measured, which allows us to save time on precise autofocusing.

Looking back, the Fourier frequency spectrum modification by a spatial filter inserted in the back focal plane of a microscope objective has been well known since Abbe's works at the end of 19th century [19]. The size selective band-pass filtering application for prescreening of cervical samples was first proposed by HUTZLER [20]. The results of his experiments showed that the signals of extended structures (*e.g.*, cytoplasm) and small objects (*e.g.*, leukocytes) were reduced to a faint background illumination. Conversely the large, atypical nuclei produced bright spots of high level intensity. A computerized system based on this idea was built in Germany by REUTER [21]. It generated signals at the positions of suspect objects but nuclei and artifacts were not differentiated which resulted in too many false alarms. The improved experimental set-up presented in this paper has been equipped with two alternative procedures for artifacts rejection.

3. Design of band-pass spatial filters

The suitable transfer characteristic of the spatial filter for measuring the nucleus diameter may be optimized by analyzing influence of the high-pass r_h and the low-pass r_l components of the filter. A mathematical simulation of the optical filtering process clearly seems to be the best way for this purpose.

It is convenient to commence by making some simplifying assumptions:

– a nucleus is regarded as a black circle of radius R_1, placed in the middle of a white circle background of radius R_2,

– the nucleus amplitude transparency and its phase retardation are equal to zero,

– the amplitude transparency of the background is set to one,

– the object is illuminated by a uniform, plane wave of the unit amplitude.

These asumptions lead to the equation describing the wave immediately past the object as

$$U(r) = \mathrm{circ}(r/R_2) - \mathrm{circ}(r/R_1) \tag{1}$$

where

$$\mathrm{circ}(r/R) = \begin{cases} 0 & r > R, \\ 1/2 & r = R, \\ 1 & r < R. \end{cases}$$

Step 1. *Fourier tansformation*

The Fourier transformation of the circ function is called the sombrero function or the Bessel sinc (Bs). Namely

$$\mathrm{FT}[\mathrm{circ}(r/R)] = 2\pi R^2 \mathrm{Bs}(2\pi R\rho) \tag{2}$$

where $\mathrm{Bs}(2\pi R\rho) = J_1(2\pi R\rho)/(2\pi R\rho)$, and J_1 is the Bessel function of the first kind, order one.

Since the transform of a sum is the sum of the transforms (linearity theorem), the distribution in the focal plane may be written

$$\mathrm{FT}[\mathrm{circ}(r/R_2) - \mathrm{circ}(r/R_1)] = \mathrm{FT}[\mathrm{circ}(r/R_2)] - \mathrm{FT}[\mathrm{circ}(r/R_1)] \tag{3}$$

and substituting from (2)

$$H(\rho) = 2\pi[R_2^2 \mathrm{Bs}(2\pi R_2\rho) - R_1^2 \mathrm{Bs}(2\pi R_1\rho)]. \tag{4}$$

Step 2. *Fourier spectrum modification*

The modified spectrum can be found from the equation

$$\mathrm{Hm}(\rho) = H(\rho)T_f(\rho) \tag{5}$$

where $T_f(\rho)$ is the band-pass filter transmittance given by

$$T_f(\rho) = \mathrm{circ}(\rho/r_1) - \mathrm{circ}(\rho/r_h). \tag{6}$$

Step 3. *Inverse Fourier transformation of the modified spectrum*

This operation has been performed numerically using the Radon transformation and the related central slice theorem (Fig. 2) [22], [23]. The latter shows that 1D Fourier transform of a line integral projection R of a 2D function $f(x, y)$ is one line (slice A) through the 2D Fourier transform of the original function. The set of projections for all azimuth angles α constitutes the Radon transform. However, the $\mathrm{Hm}(\rho)$ function is circularly symmetrical, thus only one projection and one Fourier transform is required to determine the final function.

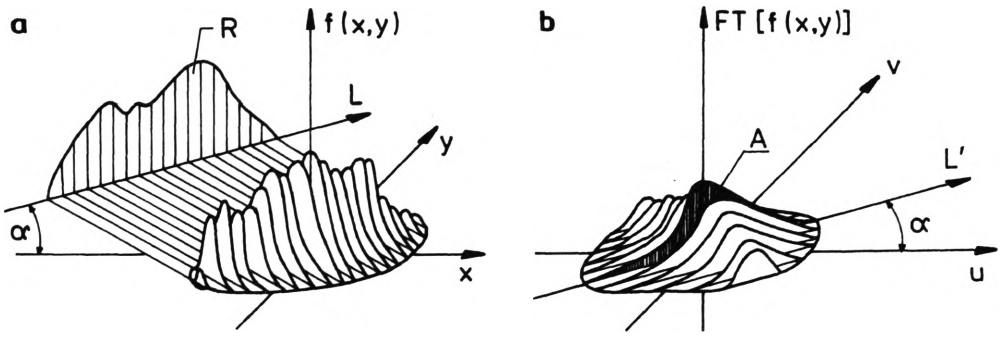

Fig. 2. Radon transform (a) and the related central slice theorem (b)

The use of the Radon–Fourier transformation makes it possible to apply FFT procedure which is very convenient, because it is easily available and is frequently hardware supported.

The simulation results demonstrate the influence of the low-pass r_l (Fig. 3) and high-pass r_h component of the filter. Intensity is measured in the centre of the object. It can be seen that decreasing r_l shifts the intensity maximum towards greater nuclei. However, when r_h component is constant, the intensity level drops dramatically.

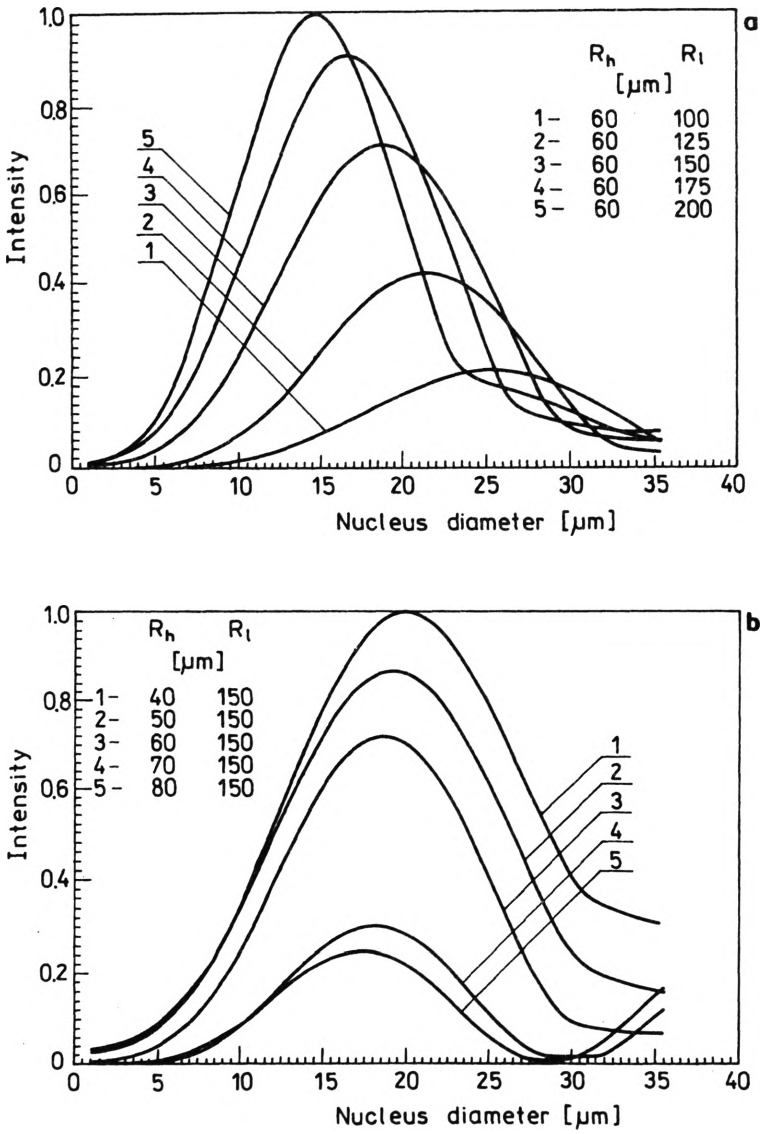

Fig. 3. Relation between intensity and low-pass (a) and high-pass (b) component of the spatial filter

Since the high-pass component determines practically only the value of intensity and has minor influence on the maximum location, its radius may be decreased. On the other hand, the central part of the filter has to cover the image of the light source. The size of the light source depends on the technique of the coherent noise suppression which is to be considered later (Sect. 6.1). Clearly, a compromise must be made to optimize the high-pass component of the filter.

4. Setup for optical filtering

The setup (Fig. 4) consists of two, partially interpenetrating channels. The first is a commercial research microscope for a visual inspection, which has a built-in illuminator based on the Köhler principle of illumination [24]. The second is designed for a coherent light source (helium-neon or diode laser). The components UF1, UF1', UF2 and a mirror ZO constitute its beam forming part, and UZ, OP, TF, ObK the filtering part. The white light beam and the laser light beams are

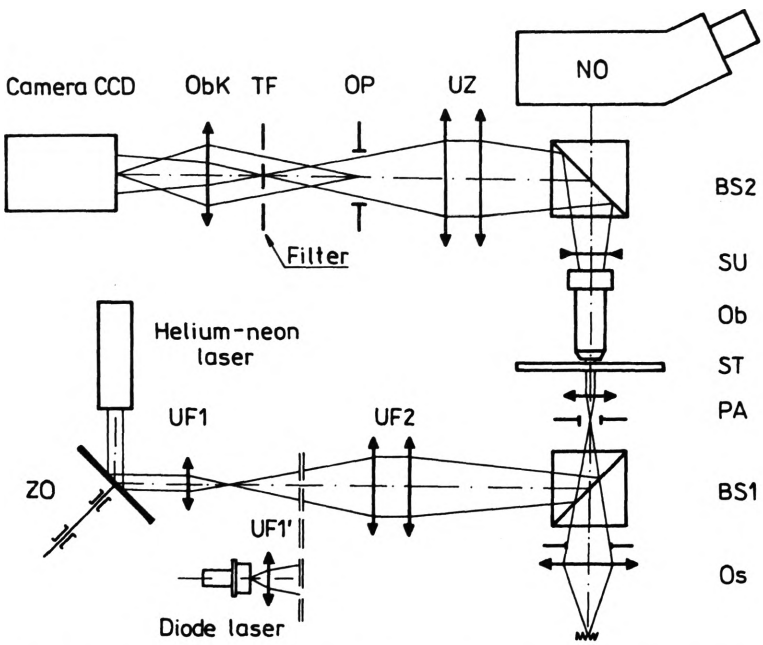

Fig. 4. Microscope based setup for optical filtering (for explanation, see the text)

combined in front of the condenser and separated after the specimen ST and the objective Ob by the polarizing cubic splitters BS1, BS2. An image – transfer unit UZ re-images the back focal plane of the objective Ob to an accessible plane TF, where spatial filter is placed. The image of the specimen is projected to infinity by the objective Ob and negative lens SU and then focused by the image transfer system UZ to an intermediate plane OP, where an auxiliary field diaphragm is inserted. The image – after being filtered – is observed through the CCD camera with its

objective ObK and is transmitted into the computer memory by the use of a framegrabber interface.

5. Specimen preparation

There are two commonly accepted staining techniques:

- hematoxylin and eosin (HE), [25],
- Papanicolau [26].

Both methods use hematoxylin for staining nuclei. Two counterstains are used in the Papanicolau technique: orange G to stain the cellular glycogen and keratin, and EA (contains eosin) to stain the cytoplasm. After applying these reagents, the cytoplasm becomes green or red depending on the stage of development of the cell and its properties. When monochromatic light is used, green cells have different gray level than red ones which results in unequal local contrast of the nucleus. Therefore, nuclei of the same diameter produce signals of a different intensity. In the HE method cytoplasm is stained pink by eosion only. Cells differ in shade only slightly and the above mentioned problem does not exist. Therefore, the HE method has been chosen.

The wavelength of laser light for the filtering procedure has been selected so that the nuclei have the highest and the cytoplasm the lowest contrast. The analysis of the spectral transmittance of eosin and hematoxylin (Fig. 5) shows that the desired value lies between 590 and 635 nm. This has been verified by further experiments on routine samples. Sufficiently good results have been achieved for red He-Ne laser (633 nm) but the latest tests have indicated that the most preferable will be the yellow He-Ne laser (594 nm).

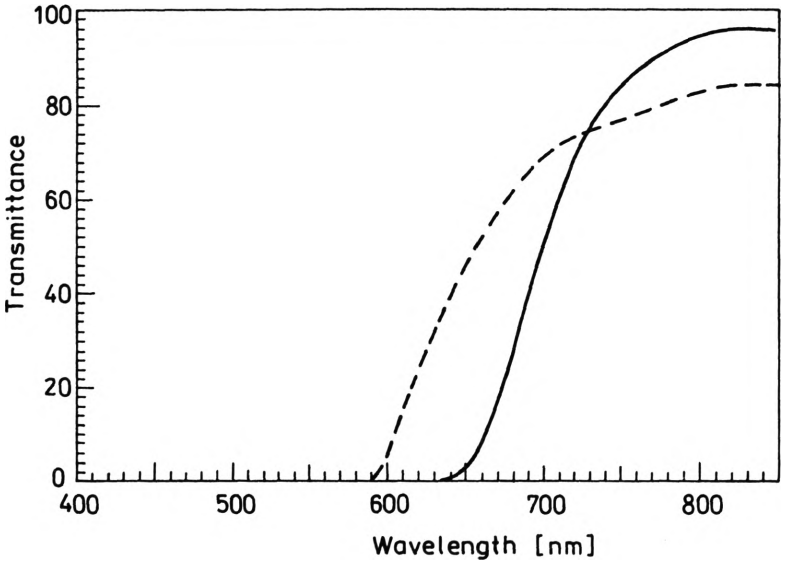

Fig. 5. Hematoxylin (solid line) and eosin spectral transmittance

The contrast of the nuclei may be enhanced by prolonging the staining process, but it must be done with care because it may smear the inner structure of the nuclei. The analysis of this structure in the HR mode is very important as well as in the case of the visual inspection by cytotechnicians. Samples should be prepared so as to have a one cell thickness, and breaking clumps is essential for successful machine processing.

6. Noise suppression techniques

6.1. Coherent noise

6.1.1. Visible lasers

The use of an He-Ne or, *e.g.*, Toshiba visible diode lasers gives a speckled background in a filtered image which is known as coherent noise. The time averaging techniques (called also "method of dynamic coherent illumination") may be applied to reduce noise [27], [28]. In these methods, parameters of the illuminating beam vary in time and as a result subsequent images differ in background. The CCD camera works as a time averaging device. Two modifications of this method have been tested. The first involves a rotating ground glass. The phase in an illuminating beam fluctuates during rotation according to the granular pattern. The second employs a rotating mirror (Fig. 4, component ZO) the axis of which is deflected from its orthogonal position in reference to the reflecting plane. As a result an image of the light source moves on a circle in the Fourier plane. The circle radius can be adjusted by changing the deflection angle. The experiments reveal that slightly better results may be obtained using the method based on a rotating ground glass.

6.1.2. Infrared diode laser

In order to reject artifacts of cervical smears (which is dealt with in detail in Sect. 6.2) filtered images in red and infrared light should be compared. The diode laser CQYP 60 ($\lambda = 890$ nm, $\Delta\lambda = 4.5$ nm) has been used as an infrared light source. It has a strongly asymmetric emitting element of size 1×250 or 2×250 μm (according to a laser version). This results in one-dimensional character of coherent noise. In the filtering system, image of the light source is demagnified twice jointly by the beam forming lenses and the microscope condenser. Band-pass filtering requires that the entire image must be covered by the central part of the spatial filter which cannot be ensured by the noise suppression techniques mentioned previously. Instead, a new method has been developed which consists in rotating the light source about its centre. A CCD camera averages the subsequent frames illuminated with the light source in its different angular orientation. Consequently, in this way averaged image is formed with the pseudo-circle source. However, because of construction difficulties the laser itself cannot be rotated. Instead, a Dove prism was used for this purpose. If the prism is rotated about its axis (the axis is determined by the ray which emerges along a continuation of its incident direction) through some angle, the image rotates through twice that angle. This feature of the prism allows lowering the rotational speed of the prism, which is convenient from the mechanical point of view.

6.1.3. Light emitting diodes (LEDs)

Searching for more convenient light sources, some experiments have been performed with Toshiba LEDs using a specially designed test plate which consisted of nine equal, opaque circles.

The LEDs of this type have a square light source of size 0.3 mm. For filtering process ony red diodes (660 nm) have sufficient high luminous intensity (7 cd, type TLRA 190P) at forward current $I_F = 20$ mA. In DC driving mode, maximum $I_F = 50$ mA. The filtering process may be performed successfully on condition that $I_F > 30$ mA. Commercially available diodes cannot be directly applied to the optical system because of their lens-like ending made of epoxy resin. In the diode used in the experiments this ending has been taken away, leaving a 0.5 mm layer of the material above the emitting structure, then the surface has been polished. Undesired reflections have been masked by the diaphragm of the source size, placed directly on a polished surface. The diode has been inserted in the front focal plane of the condenser.

Because of relatively large light source the image has been freed from coherent noise almost completely without using any additional techniques.

These undoubtedly good results of LEDs as a light source would incline us to take a much more optimistic view of the noise suppression problem if the diode emitted shorter wave. Because of spectral transmittance of reagents used for staining smears the most desirable wavelength is within range of 550–635 nm (Sect. 5) which eliminates LEDs for the time being in this application.

6.2. Phase and amplitude artifacts

Phase and amplitude objects are an additional source of noise. According to the filtering theory they produce signals of the intensities comparable or higher than those generated by nuclei, which leads to false alarms. To avoid this, two alternative techniques have been developed and tested. They employ a spectral transmittance of the stain used in sample preparation – hematoxylin. It can be seen (Fig. 5) that the stain transmittance is high for infrared light and low for the visible spectrum. Practically, a nucleus is transparent in infrared light (Fig. 1c). The first method (FD) consists in comparison between filtered and direct images recorded in visible (the most preferable is 594 nm) and infrared light (750–900 nm). A software procedure is sketched in Fig. 6 in detail. The filtered image is scanned line by line from the top to the bottom of the screen. When a pixel representing a threshold intensity level is detected, its square neighbourhood is searched to find a pixel of the maximum intensity. The coordinates of the latter are regarded as the centre of the nucleus. Then the processing is passed to the direct image in visible light to determine whether the corresponding place is a dark or white spot which is equivalent to a nucleus or amplitude artifact, and a phase object, respectively. The nucleus average intensity I_n in the circle neighbourhood of a radius r_1 and the background average intensity I_b in the annulus of radii r_2 and r_3 are calculated. Radii r_1, r_2 refer to the smallest and greatest nucleus radius, respectively. The radius r_3 has been optimized experimentally. The difference $I_b - I_n$ is a good recognition criterion. It takes large positive

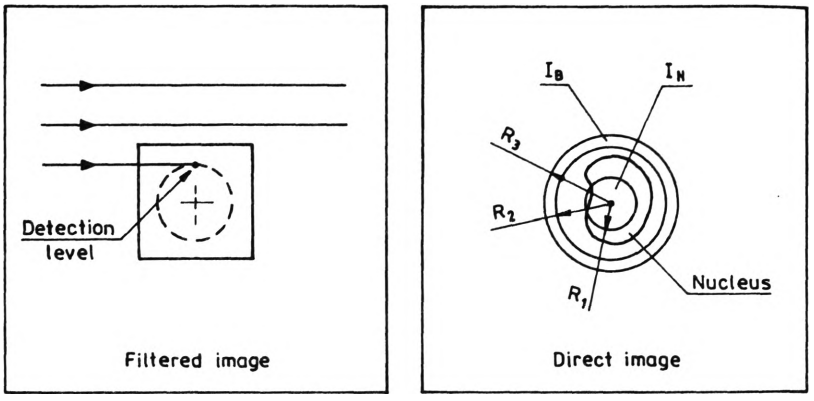

Fig. 6. Artifact rejection technique which compares filtered and direct images

values for dark spots and small positive or negative values for phase structures. If the tested object is classified as dark, the intensities I_b, I_n are recalculated for the direct image in infrared light. The intensity difference is close to zero for the nucleus and large for the amplitude artifact, because the transmittance of the latter is usually constant for a visual and infrared light.

The second method (FF) employs two filtered images in visible and infrared light. The distinguishing procedure is as follows: the image is scanned using red light (He-Ne laser 633 nm). When a signal is detected, the light source is switched to the infrared one (diode laser 890 nm). The signal level drop means that a nucleus has been found – otherwise the alarm is ignored since it is caused by the phase or amplitude artifact. The above method is very fast because no calculation is necessary but the optical system is more complex.

7. Preliminary experimental results

The experiments have involved prescreening of 60 routine samples (manually prepared) of the different stage of the disease. Five randomly selected areas have been examined in each smear excluding clumps and clusters of cells.

The system has been able to select suspicious cells properly and the overall results have been similar to those of Reuter and Schenck's system. The detection threshold of bright spots has been set on a safe level (in order not to miss any cancer cell) which resulted in some amount of normal cells recognized as suspicious. This rate, however, does not exceed 12% which is acceptable. It has been found that the signals produced by large, neighbouring nuclei may disturb each other. In a few cases this prevents them from being detected. A concentration of pathological cells, in those cases, was so great that the other cells were classified correctly. A high signal has been also generated by overlapping normal cells. All this clearly indicates that proper sample preparation is of great importance – in particular monolayer dispersion.

In contrast to Reuter and Schenck's system, the phase and amplitude artifacts (particles of dust, talc) have had no effect on the result of prescreening process. In occasional cases when a nucleus is covered by an amplitude artifact the former is rejected as an artifact. The FF method is also sensitive to phase artifact of the mentioned configuration. In such a case the bright spot does not disappear after switching into infrared laser. Coincidence in localization of artifacts and nuclei occurs very rarely and is not a potential danger.

8. Conclusions

Preliminary tests of the system have proved its ability to detect suspicious cells. Furthermore, the false alarms produced by phase objects and dark amplitude artifacts have been practically eliminated. However, the desired accuracy of prescreening the cytological samples needs further investigation. Particularly the cells overlapping must be eliminated by applying automated techniques to the sample preparation and their standardization. An additional procedure should be applied to break up clumps and clusters of cells [29]–[31].

The problem of phase (but not amplitude) artifacts could be eliminated by the use of spatial light modulators (SLM), but the limited resolution may result in relatively small processing area and the system could not be as compact as it is in its present version. Nevertheless, the idea of SLM is worth reconsideration.

Considering the above mentioned system characteristic, it can be said that the optical band-pass filtering technique speeds up the first stage of the automated processing and is an alternative technique to pure digital methods. However, clinical usefulness of the entire system needs more experiments including HR analysis. This research is in progress.

Acknowledgements – The author would like to thank Professor M. Pluta for fruitful discussion and Dr M. Daszkiewicz for his guidance and encouragement in the pursuit of these studies. Special appreciation is extended to Dr J. Galas for his assistance in the software development. Finally, the author wishes to thank Mrs J. Zamorska for her help in the samples selection. Funding in support of this research has been provided in part by the State Committee for Scientific Research (KBN), Poland, Project 800609101.

References

[1] BANDA-GAMBOA H., RICKETTS L, CAIRNS A., HUSSEIN K., TUCKER J. H., HUSAIN N., Analytical Cellular Pathology 4 (1992), 25.
[2] CHRISTOPHERSON W. M., PARKER J. E., MENDEZ W. M., LUNDIN F. E., Cancer 26 (1970), 808.
[3] BENEDET J. L., ANDERSON G. H., Gynecologic Oncology 12 (1981), 280.
[4] SOOST H. J., BOCKMUHL B., ZOCK H., Acta Cytologica 26 (1982), 445.
[5] GARUD M. A., SARAIYA U. B., LULA M., KAHN S., PARASKAR M., DAFFARY D., Acta Cytologica 27 (1983), 429.
[6] YANG D., YAO J., XING S., LIN Y., Acta Cytologica 29 (1985), 341.
[7] STENKVIST B., BERGSTRM R., EKLUND G., FOX C., J. Am. Med. Assoc. 252 (1984), 1423.
[8] ERHARDT R., REINHARDT E. R., SCHLIPF W., BLOSS W. H., Analytical & Quantitative Cytology 2 (1980), 25.

[9] PLOEM J. S., DRIEL-KULKER A. M. J., GOYARTS-VELDSTRA L., PLOEM-ZAALJER J. J., VERWOERD N. P., ZWAN M., Histochemistry **84** (1986), 549.
[10] TANAKA N., UENO T., IKEDA H., MUKAWA A., WATANABE S., OKAMOTO Y., HOSOI S., TSUNEKAWA S., Appl. Opt. **26** (1987), 3301.
[11] BENGTSSON E., ERIKSSON O., *The design of an image analysis system*, Proc. 5th Scandinavian Conference on Image Analysis, Stockholm 1987, p. 217.
[12] TAYLOR J., BARTLES P. H., BIBBO M., WIED G. L., Acta Cytologica **22** (1987), 261.
[13] PERNICK B., KOPP R. E., LISA J., MENDELSOHN J., WOLHERS R., Appl. Opt. **17** (1978), 21.
[14] TURKE B., SEGER G., ACHATZ M., SEELEN W., Appl. Opt. **17** (1978), 2754.
[15] WHEELESS L. L., PATTEN S. F., Acta Cytologica **17** (1973), 391.
[16] HARDY J. A., WHEELESS L. L., J. Histochem. Cytochem. **25** (1977), 857.
[17] WHEELESS L. L., CAMBIER J. L., CAMBIER M. A., KAY D. B., WIGHTMAN L. L., PATTEN S. F., J. Histochem. Cytochem. **27** (1979), 596.
[18] BENGTSSON E., ERIKSSON O., HOLMQUIST J., NORDIN B., STENKVIST B., J. Histochem. Cytochem. **27** (1979), 621.
[19] ABBE E. M., Arch. f. Mikroskopische Anatomie **9** (1973), 413.
[20] HUTZLER P. J. S., Appl. Opt. **16** (1977), 2264.
[21] REUTER B. W., SCHENCK U., SPIE **473** (1984), 88.
[22] BARRETT H. H., *The Radon transform and its applications*, Chapt. III, [in] *Progress in Optics*, Vol. XXI, [Ed.] E. Wolf, Elsevier Sci. Publ. B. V., 1984, pp. 219–282.
[23] TICKOR A. J., EASTON R. L., BARRETT H. H., Opt. Eng. **24** (1985), 82.
[24] PLUTA M., *Advanced Light Microscopy*, Vol. 1, *Principles and Basic Properties*, Elsevier Sci. Publ. B. V., 1988, p. 179–234.
[25] SHEEHAN C. D., HRAPCHAK B. B., *Theory and Practice of Histotechnology*, C. V. Mosby Company, Saint Louis 1973, p. 61.
[26] WHITE W. L., ERICKSON M. M., STEVENS S. C., *Practical Automation for the Clinical Laboratory*, C. V. Mosby Company, Saint Louis 1972, p. 520.
[27] THOMAS C. E., Appl. Opt. **7** (1968), 517.
[28] MRÓZ E., PAWLUCZYK R., PLUTA M., Opt. Appl. **1** (1971), 9.
[29] TANAKA N., IKEDA K., UENO T., OKAMOTO Y., HOSOI S., Analytical & Quantitative Cytology **3** (1981), 96.
[30] ROSENTHAL D. L., LEIBEL J., MEYER D. J., WOODS S. D., MCLATCHIE C., SUFFIN S. C., CASTLEMAN K. R., Analytical & Quantitative Cytology **5** (1983), 236.
[31] ROSENTHAL D. L., MANJIKIAN V., Analytical & Quantitative Cytology **9** (1987), 55.

Received June 1, 1994